

Evidence for $B^- \rightarrow \tau^- \bar{\nu}_\tau$ with a Semileptonic Tagging Method

K. Hara,²⁴ T. Iijima,²⁴ H. Aihara,⁴⁵ V. Aulchenko,^{1,33} T. Aushev,^{19,12} T. Aziz,⁴⁰ A. M. Bakich,³⁹
E. Barberio,²³ K. Belous,¹¹ M. Bischofberger,²⁵ A. Bondar,^{1,33} A. Bozek,²⁹ M. Bračko,^{21,13} T. E. Browder,⁷
P. Chang,²⁸ Y. Chao,²⁸ A. Chen,²⁶ B. G. Cheon,⁶ C.-C. Chiang,²⁸ I.-S. Cho,⁴⁹ Y. Choi,³⁸ J. Dalseno,^{22,41}
M. Danilov,¹² Z. Doležal,² W. Dungel,¹⁰ S. Eidelman,^{1,33} N. Gabyshev,^{1,33} P. Goldenzweig,⁴ B. Golob,^{20,13}
H. Ha,¹⁷ Y. Hasegawa,³⁷ K. Hayasaka,²⁴ H. Hayashii,²⁵ Y. Horii,⁴⁴ Y. Hoshi,⁴³ Y. B. Hsiung,²⁸ H. J. Hyun,¹⁸
K. Inami,²⁴ M. Iwabuchi,⁴⁹ Y. Iwasaki,⁸ T. Julius,²³ J. H. Kang,⁴⁹ H. Kawai,³ T. Kawasaki,³¹ H. Kichimi,⁸
C. Kiesling,²² H. J. Kim,¹⁸ H. O. Kim,¹⁸ J. H. Kim,¹⁶ M. J. Kim,¹⁸ Y. J. Kim,⁵ K. Kinoshita,⁴ B. R. Ko,¹⁷
P. Kodyš,² S. Korpar,^{21,13} M. Kreps,¹⁵ P. Križan,^{20,13} P. Krokovny,⁸ T. Kuhr,¹⁵ T. Kumita,⁴⁶ A. Kuzmin,^{1,33}
Y.-J. Kwon,⁴⁹ S.-H. Kyeong,⁴⁹ M. J. Lee,³⁶ S.-H. Lee,¹⁷ J. Li,⁷ A. Limosani,²³ Y. Liu,²⁸ D. Liventsev,¹²
R. Louvot,¹⁹ A. Matyja,²⁹ S. McOnie,³⁹ K. Miyabayashi,²⁵ H. Miyata,³¹ Y. Miyazaki,²⁴ G. B. Mohanty,⁴⁰
T. Mori,²⁴ E. Nakano,³⁴ M. Nakao,⁸ H. Nakazawa,²⁶ S. Neubauer,¹⁵ S. Nishida,⁸ K. Nishimura,⁷ O. Nitoh,⁴⁷
T. Nozaki,⁸ S. Ogawa,⁴² T. Ohshima,²⁴ S. Okuno,¹⁴ S. L. Olsen,^{36,7} H. Ozaki,⁸ G. Pakhlova,¹² C. W. Park,³⁸
H. K. Park,¹⁸ R. Pestotnik,¹³ M. Petrič,¹³ L. E. Piilonen,⁴⁸ M. Prim,¹⁵ M. Rozanska,²⁹ S. Ryu,³⁶ H. Sahoo,⁷
Y. Sakai,⁸ O. Schneider,¹⁹ J. Schümann,⁸ C. Schwanda,¹⁰ A. J. Schwartz,⁴ K. Senyo,²⁴ M. E. Sevier,²³
M. Shapkin,¹¹ H. Shibuya,⁴² J.-G. Shiu,²⁸ B. Shwartz,^{1,33} J. B. Singh,³⁵ P. Smerkol,¹³ E. Solovieva,¹² S. Stanič,³²
M. Starič,¹³ K. Sumisawa,⁸ T. Sumiyoshi,⁴⁶ Y. Teramoto,³⁴ I. Tikhomirov,¹² K. Trabelsi,⁸ S. Uehara,⁸
T. Uglov,¹² Y. Unno,⁶ S. Uno,⁸ Y. Ushiroda,⁸ G. Varner,⁷ K. E. Varvell,³⁹ K. Vervink,¹⁹ C. H. Wang,²⁷
M.-Z. Wang,²⁸ P. Wang,⁹ Y. Watanabe,¹⁴ R. Wedd,²³ E. Won,¹⁷ B. D. Yabsley,³⁹ Y. Yamashita,³⁰
M. Yamauchi,⁸ C. Z. Yuan,⁹ C. C. Zhang,⁹ V. Zhilich,^{1,33} T. Zivko,¹³ A. Zupanc,¹⁵ and O. Zyukova^{1,33}

(The Belle Collaboration)

¹*Budker Institute of Nuclear Physics, Novosibirsk*

²*Faculty of Mathematics and Physics, Charles University, Prague*

³*Chiba University, Chiba*

⁴*University of Cincinnati, Cincinnati, Ohio 45221*

⁵*The Graduate University for Advanced Studies, Hayama*

⁶*Hanyang University, Seoul*

⁷*University of Hawaii, Honolulu, Hawaii 96822*

⁸*High Energy Accelerator Research Organization (KEK), Tsukuba*

⁹*Institute of High Energy Physics, Chinese Academy of Sciences, Beijing*

¹⁰*Institute of High Energy Physics, Vienna*

¹¹*Institute of High Energy Physics, Protvino*

¹²*Institute for Theoretical and Experimental Physics, Moscow*

¹³*J. Stefan Institute, Ljubljana*

¹⁴*Kanagawa University, Yokohama*

¹⁵*Institut für Experimentelle Kernphysik, Karlsruher Institut für Technologie, Karlsruhe*

¹⁶*Korea Institute of Science and Technology Information, Daejeon*

¹⁷*Korea University, Seoul*

¹⁸*Kyungpook National University, Taegu*

¹⁹*École Polytechnique Fédérale de Lausanne (EPFL), Lausanne*

²⁰*Faculty of Mathematics and Physics, University of Ljubljana, Ljubljana*

²¹*University of Maribor, Maribor*

²²*Max-Planck-Institut für Physik, München*

²³*University of Melbourne, School of Physics, Victoria 3010*

²⁴*Nagoya University, Nagoya*

²⁵*Nara Women's University, Nara*

²⁶*National Central University, Chung-li*

²⁷*National United University, Miao Li*

²⁸*Department of Physics, National Taiwan University, Taipei*

²⁹*H. Niewodniczanski Institute of Nuclear Physics, Krakow*

³⁰*Nippon Dental University, Niigata*

³¹*Niigata University, Niigata*

³²*University of Nova Gorica, Nova Gorica*

³³*Novosibirsk State University, Novosibirsk*

³⁴*Osaka City University, Osaka*

³⁵*Panjab University, Chandigarh*³⁶*Seoul National University, Seoul*³⁷*Shinshu University, Nagano*³⁸*Sungkyunkwan University, Suwon*³⁹*School of Physics, University of Sydney, NSW 2006*⁴⁰*Tata Institute of Fundamental Research, Mumbai*⁴¹*Excellence Cluster Universe, Technische Universität München, Garching*⁴²*Toho University, Funabashi*⁴³*Tohoku Gakuin University, Tagajo*⁴⁴*Tohoku University, Sendai*⁴⁵*Department of Physics, University of Tokyo, Tokyo*⁴⁶*Tokyo Metropolitan University, Tokyo*⁴⁷*Tokyo University of Agriculture and Technology, Tokyo*⁴⁸*IPNAS, Virginia Polytechnic Institute and State University, Blacksburg, Virginia 24061*⁴⁹*Yonsei University, Seoul*

We present a measurement of the decay $B^- \rightarrow \tau^- \bar{\nu}_\tau$ using a data sample containing 657×10^6 $B\bar{B}$ pairs collected at the $\Upsilon(4S)$ resonance with the Belle detector at the KEKB asymmetric-energy e^+e^- collider. A sample of B^+B^- pairs are tagged by reconstructing one B^+ meson decaying semileptonically. We detect the $B^- \rightarrow \tau^- \bar{\nu}_\tau$ candidate in the recoil. We obtain a signal with a significance of 3.6 standard deviations including systematic uncertainties, and measure the branching fraction to be $\mathcal{B}(B^- \rightarrow \tau^- \bar{\nu}_\tau) = [1.54_{-0.37}^{+0.38}(\text{stat})_{-0.31}^{+0.29}(\text{syst})] \times 10^{-4}$. This result confirms the evidence for $B^- \rightarrow \tau^- \bar{\nu}_\tau$ obtained in a previous Belle measurement that used a hadronic B tagging method.

PACS numbers: 13.20.He, 14.40.Nd

The purely leptonic decay $B^- \rightarrow \tau^- \bar{\nu}_\tau$ [1] is of particular interest since it provides a unique opportunity to test the Standard Model (SM) and search for new physics beyond the SM. In the SM, the branching fraction of the decay $B^- \rightarrow \tau^- \bar{\nu}_\tau$ is given by

$$\mathcal{B}(B^- \rightarrow \tau^- \bar{\nu}_\tau) = \frac{G_F^2 m_B m_\tau^2}{8\pi} \left(1 - \frac{m_\tau^2}{m_B^2}\right)^2 f_B^2 |V_{ub}|^2 \tau_B, \quad (1)$$

where G_F is the Fermi coupling constant, m_τ and m_B are the τ lepton and B^- meson masses, τ_B is the B^- lifetime, $|V_{ub}|$ is the magnitude of the Cabibbo-Kobayashi-Maskawa (CKM) matrix element [2], and f_B is the B meson decay constant. Dependence on the lepton mass arises from helicity conservation, which suppresses the muon and electron channels. A recent SM estimation of the branching fraction [3] is $(0.76_{-0.06}^{+0.11}) \times 10^{-4}$. In the absence of new physics, measurement of the $B^- \rightarrow \tau^- \bar{\nu}_\tau$ decay can provide a direct experimental determination of f_B , which can be compared to lattice QCD calculations [4]. Physics beyond the SM, however, could significantly suppress or enhance $\mathcal{B}(B^- \rightarrow \tau^- \bar{\nu}_\tau)$ via exchange of a new charged particle such as a charged Higgs boson from supersymmetry or two-Higgs doublet models [5, 6].

Belle previously reported [7] the first evidence of $B^- \rightarrow \tau^- \bar{\nu}_\tau$ decay with a significance of 3.5 standard deviations (σ), and measured the branching fraction to be $\mathcal{B}(B^- \rightarrow \tau^- \bar{\nu}_\tau) = (1.79_{-0.49}^{+0.56}(\text{stat})_{-0.51}^{+0.46}(\text{syst})) \times 10^{-4}$, using a hadronic reconstruction tagging method. The BaBar Collaboration reported a search for $B^- \rightarrow \tau^- \bar{\nu}_\tau$ decay with hadronic tagging [8] using 383×10^6 $B\bar{B}$ pairs and with semileptonic tagging [9] using 459×10^6 $B\bar{B}$ pairs. Combining the two measurements, they obtained

a 2.8σ excess and a branching fraction $\mathcal{B}(B^- \rightarrow \tau^- \bar{\nu}_\tau) = (1.7 \pm 0.6) \times 10^{-4}$. These experimental results are slightly larger than the SM estimation in Ref. [3], though the statistical precision is not sufficient to demonstrate the existence of physics beyond the SM. To better establish this decay mode and determine the branching fraction with greater precision, we present a measurement of $B^- \rightarrow \tau^- \bar{\nu}_\tau$ from Belle using a semileptonic tagging method.

We use a 605 fb^{-1} data sample containing 657×10^6 $B\bar{B}$ pairs collected with the Belle detector at the KEKB asymmetric-energy e^+e^- (3.5 on 8 GeV) collider [10] operating at the $\Upsilon(4S)$ resonance ($\sqrt{s} = 10.58 \text{ GeV}$). We also use a data sample of 68 fb^{-1} taken at a center of mass energy 60 MeV below the nominal $\Upsilon(4S)$ mass (off-resonance) for background studies. The Belle detector [11] is a large-solid-angle magnetic spectrometer that consists of a silicon vertex detector (SVD), a 50-layer central drift chamber (CDC), an array of aerogel threshold Cherenkov counters (ACC), a barrel-like arrangement of time-of-flight scintillation counters (TOF), and an electromagnetic calorimeter (ECL) comprised of CsI(Tl) crystals located inside a superconducting solenoid coil that provides a 1.5 T magnetic field. An iron flux-return located outside of the coil is instrumented to detect K_L^0 mesons and to identify muons (KLM). Two inner detector configurations were used. A 2.0 cm beampipe and a 3-layer silicon vertex detector were used for the first sample of 152×10^6 $B\bar{B}$ pairs, while a 1.5 cm beampipe, a 4-layer silicon detector and a small-cell inner drift chamber were used to record the remaining 505×10^6 $B\bar{B}$ pairs [12].

We use a detailed Monte Carlo (MC) simulation based

on GEANT [13] to determine the signal selection efficiency and study the background. In order to reproduce the effects of beam background, data taken with random triggers for each run period are overlaid on simulated events. The $B^- \rightarrow \tau^- \bar{\nu}_\tau$ signal decay is generated by the EvtGen package [14]. Radiative effects are modeled using the PHOTOS code [15]. To model the background from $e^+e^- \rightarrow B\bar{B}$ and continuum $q\bar{q}$ ($q = u, d, s, c$) production processes, we use large MC samples of $B\bar{B}$ meson pair decays to charm and continuum $q\bar{q}$ processes corresponding to about ten times and six times the data sample, respectively. We also use MC samples of rare B decay processes such as charmless hadronic, radiative, electroweak decays and $b \rightarrow u$ semileptonic decays. The contamination from other low multiplicity backgrounds such as $e^+e^- \rightarrow \tau^+\tau^-$ and two-photon processes is also studied using dedicated MC samples.

The $B^- \rightarrow \tau^- \bar{\nu}_\tau$ candidate decays are selected using the feature that at the $\Upsilon(4S)$ resonance B meson pairs are produced with no additional particles. We first reconstruct one of the B mesons decaying semileptonically (referred to hereafter as B_{tag}) and then compare the properties of the remaining particle(s) in the event (B_{sig}) to those expected for signal and background. In order to avoid experimental bias, the signal region in data is not examined until the event selection criteria are finalized.

Charged particles are selected from well measured tracks (reconstructed with the CDC and SVD) originating from the interaction point. Electron candidates are identified based on a likelihood calculated using the following information: dE/dx measured in the CDC, the response of the ACC, the ECL shower shape and the ratio of the ECL energy deposited to the track momentum. Muon candidates are selected using KLM hits associated to a charged track. Both muons and electrons are selected with efficiency greater than 90% in the momentum region above 1.2 GeV/c, and misidentification rates of less than 0.2% (1.5%) for electrons (muons). After selecting leptons, we distinguish charged kaons from pions based on a kaon likelihood derived from the TOF, ACC, and dE/dx measurements in the CDC. The typical kaon identification efficiency is greater than 85% and the probability of misidentifying pions as kaons is about 8%. Photons are identified as isolated ECL clusters that are not matched to any charged track. Neutral π^0 candidates are selected from pairs of photons with invariant mass between 0.118 and 0.150 GeV/c². The energy of the photon candidates must exceed: 50 MeV for the barrel, 100 MeV for the forward endcap and 150 MeV for the backward endcap, except for low momentum π^0 candidates from $\bar{D}^{*0} \rightarrow \bar{D}^0 \pi^0$ decay for which we require the photon energy to be greater than 30 MeV.

We reconstruct the B_{tag} in $B^+ \rightarrow \bar{D}^{*0} \ell^+ \nu_\ell$ and $B^+ \rightarrow \bar{D}^0 \ell^+ \nu_\ell$ decays, where ℓ is electron (e) or muon (μ). \bar{D}^0 mesons are reconstructed in the $K^+\pi^-$, $K^+\pi^-\pi^0$ and

$K^+\pi^-\pi^+\pi^-$ modes. For B_{sig} , we use τ^- decays to only one charged particle and neutrinos i.e. $\tau^- \rightarrow \ell^- \bar{\nu}_\ell \nu_\tau$ and $\tau^- \rightarrow \pi^- \nu_\tau$.

We require the invariant mass of \bar{D}^0 candidates to be in the range [1.851 GeV/c², 1.879 GeV/c²] for $\bar{D}^0 \rightarrow K^+\pi^-$ and $K^+\pi^-\pi^+\pi^-$ decays, and [1.829 GeV/c², 1.901 GeV/c²] for $\bar{D}^0 \rightarrow K^+\pi^-\pi^0$ decay. \bar{D}^{*0} candidates are selected by combining the \bar{D}^0 candidates with low momentum π^0 candidates or photons. For \bar{D}^{*0} candidates, we require the mass difference $\Delta M \equiv M_{D^{*0}} - M_{D^0}$ to be in the range [0.1389 GeV/c², 0.1455 GeV/c²] and [0.123 GeV/c², 0.165 GeV/c²] for $\bar{D}^{*0} \rightarrow \bar{D}^0 \pi^0$ and $\bar{D}^{*0} \rightarrow \bar{D}^0 \gamma$ decays, respectively. These regions correspond to three standard deviations in the corresponding resolutions. To suppress \bar{D}^{*0} 's from continuum background processes, the momentum of \bar{D}^{*0} candidates calculated in the $\Upsilon(4S)$ center-of-mass system (cms) is required to be less than 2.5 GeV/c.

We select signal candidates from events with one \bar{D}^0 or \bar{D}^{*0} and one ℓ^+ to form B_{tag} , and one ℓ^- or π^- candidate for B_{sig} . We require that no other charged particle or π^0 remain in the event after removing the particles from the B_{tag} and B_{sig} candidates. The B_{tag} candidates are selected using the lepton momentum in the cms frame, P_ℓ^{cms} , and the cosine of the angle between the direction of the B_{tag} momentum and the direction of the momentum sum of the $\bar{D}^{(*)0}$ and the lepton, $\cos \theta_{B, D^{(*)}\ell}$, measured in the cms frame. This angle is calculated using

$$\cos \theta_{B, D^{(*)}\ell} = \frac{2E_{\text{beam}}^{\text{cms}} E_{D^{(*)}\ell}^{\text{cms}} - m_B^2 - M_{D^{(*)}\ell}^2}{2P_B^{\text{cms}} \cdot P_{D^{(*)}\ell}^{\text{cms}}}, \quad (2)$$

where $E_{\text{beam}}^{\text{cms}}$ is the beam energy, P_B^{cms} is the momentum of B meson calculated with $P_B^{\text{cms}} = \sqrt{(E_{\text{beam}}^{\text{cms}})^2 - m_B^2}$, $E_{D^{(*)}\ell}^{\text{cms}}$, $P_{D^{(*)}\ell}^{\text{cms}}$ and $M_{D^{(*)}\ell}$ are the energy sum, momentum sum and invariant mass, respectively, of the $\bar{D}^{(*)0}$ and lepton system. All parameters are calculated in the cms. Properly reconstructed B_{tag} candidates are populated within the physical range $[-1, 1]$, while combinatorial backgrounds can take unphysical values. For the signal side, the ℓ^- or π^- candidate from the τ decay is selected using the momentum in the cms, denoted $P_{\text{sig}}^{\text{cms}}$. The signal yield is obtained by fitting the distribution of the remaining energy in the ECL, denoted E_{ECL} , which is the sum of the energies of ECL clusters that are not associated with particles from the B_{tag} and B_{sig} candidates; here the E_{ECL} clusters satisfy the same minimum energy requirements as photon candidates. For signal events, E_{ECL} must be either zero or a small value arising from spillover showers created by B_{tag} and B_{sig} particles and residual beam background hits. Therefore, signal events peak at low E_{ECL} . On the other hand, background events are distributed toward higher E_{ECL} due to the contribu-

tion from additional particles. The selection criteria for P_{ℓ}^{cms} , $\cos\theta_{B,D^{(*)}\ell}$ and $P_{\text{sig}}^{\text{cms}}$ are optimized for each of the τ decay modes, because the background levels and the background components are mode-dependent. The optimization is done so that the figure of merit $s/\sqrt{s+n}$ is maximized, where s and n are the number of signal and background events expected in the signal-enhanced region $E_{\text{ECL}} < 0.2$ GeV, calculated assuming a signal branching fraction of 1.79×10^{-4} . For leptonic τ decays, the dominant background is from $B\bar{B}$ events tagged by a semileptonic decay with a correctly reconstructed combination of a \bar{D}^{*0} and a ℓ^+ . For these decays loose selection criteria are chosen to maintain high signal efficiency: $0.5 \text{ GeV}/c < P_{\ell}^{\text{cms}} < 2.5 \text{ GeV}/c$, $-2.1 < \cos\theta_{B,D^{*}\ell} < 1.3$ for the \bar{D}^{*0} mode or $-2.6 < \cos\theta_{B,D\ell} < 1.2$ for the \bar{D}^0 mode, and $0.3 \text{ GeV}/c < P_{\text{sig}}^{\text{cms}}$. For the hadronic τ decay mode, there is more background from $e^+e^- \rightarrow q\bar{q}$ continuum and combinatorial $D^{(*)0}\ell$ background. Tighter criteria are used to reduce such backgrounds: $1.0 \text{ GeV}/c < P_{\ell}^{\text{cms}} < 2.2 \text{ GeV}/c$, $-1.1 < \cos\theta_{B,D^{(*)0}\ell} < 1.1$, and $1.0 \text{ GeV}/c < P_{\text{sig}}^{\text{cms}} < 2.4 \text{ GeV}/c$. The upper bound on $P_{\text{sig}}^{\text{cms}}$ is introduced to reject two-body B decays. In addition, we suppress continuum background by requiring the cosine of the angle between the signal side pion track and the thrust axis of the B_{tag} , $\cos\theta_{\text{thr}}$, to be less than 0.9. We select candidate events in the range $E_{\text{ECL}} < 1.2$ GeV for further analysis. The number of candidate events are 2481 for $\tau^- \rightarrow e^- \bar{\nu}_e \nu_{\tau}$, 2011 for $\tau^- \rightarrow \mu^- \bar{\nu}_{\mu} \nu_{\tau}$ and 1018 for $\tau^- \rightarrow \pi^- \nu_{\tau}$ decays. Figure 1 shows the $\cos\theta_{B,D^{(*)}\ell}$ distribution for the signal candidate events including both leptonic and hadronic τ decay modes with all selection criteria other than $\cos\theta_{B,D^{(*)}\ell}$ applied. The excess over the MC expectation for events without $B \rightarrow D^{(*)}\ell\nu$ decays indicates that the final sample contains candidate events with the correct combination of a $\bar{D}^{(*)0}$ and a ℓ^+ forming a B_{tag} . In the remaining candidates, according to a MC study, 4.6%, 13.4% and 12.0% are events without a B_{tag} from B^+B^- , $B^0\bar{B}^0$ and non- $B\bar{B}$ processes, respectively.

The number of signal events is extracted from an extended maximum likelihood fit to the E_{ECL} distribution of the candidate events. Probability density functions (PDFs) for each τ decay mode are constructed from the MC simulation. We use E_{ECL} histograms obtained from MC samples for each of the signal and the background components. The PDFs are combined into a likelihood function,

$$\mathcal{L} = \frac{e^{-\sum_j n_j}}{N!} \prod_{i=1}^N \sum_j n_j f_j(E_i) \quad (3)$$

where j is an index for the signal and background contributions, n_j and f_j are the yield and the PDF, respectively, of the j th component, E_i is the E_{ECL} value in the i th event, and N is the total number of events in the

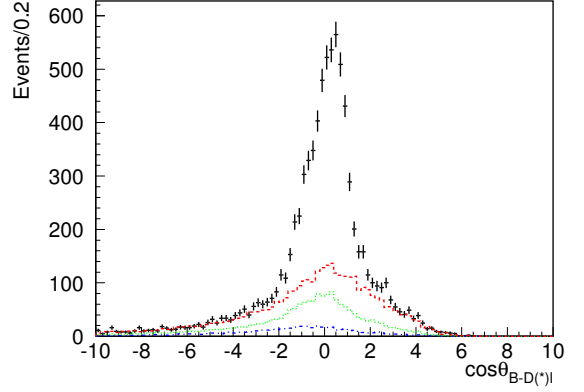


FIG. 1: $\cos\theta_{B,D^{(*)}\ell}$ distribution for candidate events with $E_{\text{ECL}} < 1.2$ GeV selected with all B_{tag} and B_{sig} requirements except for those on $\cos\theta_{B,D^{(*)}\ell}$. Leptonic and hadronic τ decay modes are combined. The points with error bars are data. The dot-dashed, dotted and dashed histograms are the MC expectation for events without $B^+ \rightarrow \bar{D}^{(*)0}\ell^+\nu_{\ell}$ decays for B^+B^- , sum of B^+B^- and $B^0\bar{B}^0$, and sum of $B\bar{B}$ and non- $B\bar{B}$ events, respectively.

data. The dominant background components are from $B\bar{B}$ decays to a final state with charm and continuum processes. The small background from rare charmless B decays and other low multiplicity processes such as τ pair and two-photon processes is also included in the fit. In the final sample with $E_{\text{ECL}} < 1.2$ GeV, the fractions of the background from rare charmless B decays and low multiplicity non- B processes are estimated from MC to be 8% and 3% for leptonic τ decays and 11% and 8% for hadronic τ decay, respectively.

The E_{ECL} estimation in MC is validated using various control samples. The MC distributions of not only E_{ECL} but also P_{ℓ}^{cms} , $\cos\theta_{B,D^{(*)}\ell}$, $P_{\text{sig}}^{\text{cms}}$ and $\cos\theta_{\text{thr}}$ are compared to those of the control samples to confirm that MC describes the background composition properly. The off-resonance data is used to calibrate the MC simulation of the continuum background. We find that our MC underestimates the overall normalization of the continuum background though the predicted shapes are consistent with data within statistical errors. We obtain the correction factor for the overall normalization of the continuum MC to be 1.43 ± 0.11 by comparing the number of remaining events in off-resonance data with the MC expectation. The sidebands in $\cos\theta_{B,D^{(*)}\ell}$, \bar{D}^{*0} mass, the mass difference between \bar{D}^{*0} and \bar{D}^0 , and E_{ECL} are used as control samples to check the overall background description including the $B\bar{B}$ contribution. The distributions in these variables obtained from MC with the continuum normalization correction applied are found to be consistent with the corresponding distributions in data.

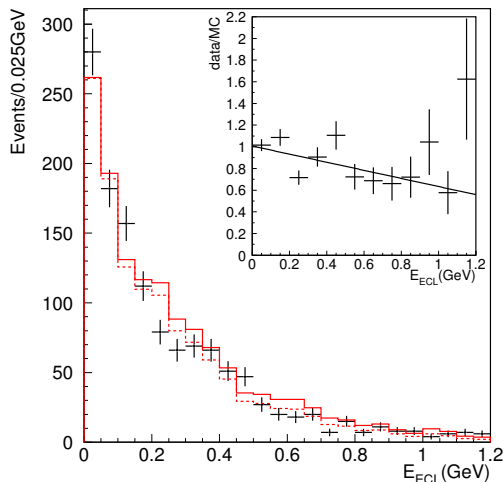


FIG. 2: E_{ECL} distribution for double semileptonic tagged events. The points with error bars are data and the solid histogram is the MC expectation scaled to the luminosity of the data. The dashed histogram is the MC expectation multiplied by the correction function described in the text. The inset shows the ratio of data to the MC expectation and the correction function.

The agreement between MC and data is also confirmed in B^0 tagged events where the B_{tag} is reconstructed in $B^0 \rightarrow D^{*-}\ell^+\nu$ decays. The contributions to the E_{ECL} distribution are not only from beam background but also include splitoff showers originating from B_{tag} and B_{sig} decay products. The relative fractions of these sources are 21%, 53% and 26%, respectively, in the signal MC sample. To take into account the possible difference between MC and data descriptions of splitoff showers, the signal E_{ECL} shape is calibrated using double tagged events, in which the B_{tag} is reconstructed in a semileptonic decay as described above and B_{sig} is reconstructed in the decay chain, $B^- \rightarrow D^{*0}\ell^-\bar{\nu}$ ($D^{*0} \rightarrow D^0\pi^0$), followed by $D^0 \rightarrow K^-\pi^+$. Figure 2 shows the E_{ECL} distribution in the double tagged sample for data and for the MC simulation scaled to the same luminosity. The background in this control sample is negligibly small. We find the E_{ECL} distribution of data tends to have a slightly smaller width than MC. The difference between the data and MC is parameterized as a first-order polynomial function of E_{ECL} obtained by fitting the ratio of data to MC for the E_{ECL} histograms of the double tagged sample. The ratio and the fit result are also shown in Fig. 2. The E_{ECL} histogram obtained from the signal MC sample is multiplied by this correction function.

In the final fit, four parameters are allowed to vary: the total signal yield and the sum of $B\bar{B}$ and continuum backgrounds for each τ decay mode. The ratio of the $B\bar{B}$ to the continuum background is fixed to the

value obtained from MC with the normalization correction applied. Other background contributions are fixed to the MC expectation. We combine τ decay modes by constraining the ratios of the signal yields to the ratio of the reconstruction efficiencies obtained from MC including the branching fractions of τ decays [16]. Figure 3 shows the E_{ECL} distribution overlaid with the fit results. The E_{ECL} distribution for each τ decay mode is also shown. We see a clear excess of signal events in the region near zero and obtain a signal yield of $n_s = 143^{+36}_{-35}$. The branching fraction is calculated as $\mathcal{B} = n_s / (2\varepsilon N_{B^+B^-})$, where ε is the reconstruction efficiency including the branching fraction of the τ decay mode and $N_{B^+B^-}$ is the number of $\Upsilon(4S) \rightarrow B^+B^-$ events, assuming $N_{B^+B^-} = N_{B^0\bar{B}^0}$. Table I lists the signal yields and the branching fractions obtained from separate fits to each τ decay mode and the fit with all three modes combined. The results of the individual fits are consistent within statistics. The χ^2 of the three results is 2.43 for two degrees of freedom, corresponding to a 30% confidence level.

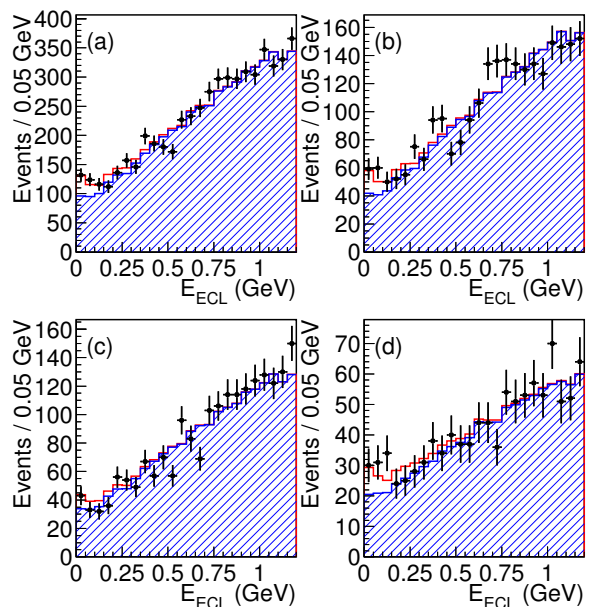


FIG. 3: E_{ECL} distribution of semileptonic tagged events with the fit result for (a) all τ decay modes combined, (b) $\tau^- \rightarrow e^- \bar{\nu}_e \nu_\tau$, (c) $\tau^- \rightarrow \mu^- \bar{\nu}_\mu \nu_\tau$ and (d) $\tau^- \rightarrow \pi^- \nu_\tau$. The points with error bars are data. The hatched histogram and solid open histogram are the background and the signal contributions, respectively.

Systematic errors for the measured branching fraction are associated with the uncertainties in the signal yield, efficiencies and the number of B^+B^- pairs. Unless explicitly stated otherwise, the systematic errors for each

TABLE I: Results of the fit for signal yields and branching fractions. ε is the reconstruction efficiency including the branching fraction of the τ decay mode. The first error in the branching fraction is statistical and the second is systematic.

Decay Mode	Signal Yield	$\varepsilon, 10^{-4}$	$\mathcal{B}, 10^{-4}$
$\tau^- \rightarrow e^- \bar{\nu}_e \nu_\tau$	73^{+23}_{-22}	5.9	$1.90^{+0.59+0.33}_{-0.57-0.35}$
$\tau^- \rightarrow \mu^- \bar{\nu}_\mu \nu_\tau$	12^{+18}_{-17}	3.7	$0.50^{+0.76+0.18}_{-0.72-0.21}$
$\tau^- \rightarrow \pi^- \nu_\tau$	55^{+21}_{-20}	4.7	$1.80^{+0.69+0.36}_{-0.66-0.37}$
Combined	143^{+36}_{-35}	14.3	$1.54^{+0.38+0.29}_{-0.37-0.31}$

source are obtained by varying the corresponding parameters individually by their uncertainties, repeating the fit procedure and adding differences from the nominal result in quadrature. The systematic errors for the signal yield arise from the uncertainties in the PDF shapes for the signal and for the background. The uncertainty in the signal shape correction function is estimated by changing the parameters of the correction function by their errors and replacing the function with a second-order polynomial ($^{+1.9\%}_{-2.4\%}$). The systematic error from MC statistics is evaluated by varying the content of each bin in the signal E_{ECL} PDF histograms by its statistical uncertainty ($\pm 0.9\%$). The main contributions to the systematic errors for the background PDF shapes are statistical errors in the MC histograms ($^{+8.6\%}_{-8.3\%}$), which is estimated in the same way as the signal PDF MC statistical uncertainty. Other large sources are the uncertainties in the background composition. The errors due to the uncertainties in the branching fractions of B decay modes that peak near zero E_{ECL} such as $B^- \rightarrow D^0 \ell^- \bar{\nu}_\ell$ with $D^0 \rightarrow K_L^0 K_L^0$, $K_L^0 \pi^0$ and $K^- \ell^+ \nu_\ell$, and $\bar{B}^0 \rightarrow D^+ \ell^- \bar{\nu}_\ell$ with $D^+ \rightarrow K_L^0 \ell^+ \nu_\ell$ are estimated by changing the branching fractions in MC by their errors [16] ($^{+4.5\%}_{-8.8\%}$). For branching fractions of D decays with a K_L^0 , we use the values for the corresponding D decays with K_S^0 's. Uncertainties in the background from the possible contribution of rare charmless B decays such as $B^- \rightarrow \pi^0 \ell^- \bar{\nu}_\ell$, $B^- \rightarrow K^- \nu \bar{\nu}$ and $\ell^- \bar{\nu}_\ell \gamma$, and from $\tau^+ \tau^-$ pair and two photon processes are evaluated by changing the fractions obtained from MC by their experimental errors [16] if available, or by $\pm 50\%$ otherwise ($^{+7.6\%}_{-7.7\%}$). The systematic error due to the uncertainty in the normalization correction factor for the continuum MC is $^{+2.6\%}_{-2.5\%}$. The systematic error associated with the reconstruction efficiency of the tag-side B is evaluated by comparing of the $\mathcal{B}(B^- \rightarrow D^{*0} \ell^- \bar{\nu}_\ell)$ branching fraction measured with the double tagged sample in data to the world average value [16]. We obtain the ratio to be 0.907 ± 0.044 and take the difference from unity plus one σ as the systematic error (13.7%). The systematic errors in the signal-side efficiencies arise from the uncertainty in tracking efficiency (1.0%), particle identification efficiency (1.3%), branching fractions of τ decays (0.4%), and MC statistics

(0.8%). The systematic error due to the uncertainty in $N_{B^+B^-}$ is 1.4%. The total fractional systematic uncertainty is $^{+19\%}_{-20\%}$, and the branching fraction is

$$\mathcal{B}(B^- \rightarrow \tau^- \bar{\nu}_\tau) = (1.54^{+0.38}_{-0.37}(\text{stat})^{+0.29}_{-0.31}(\text{syst})) \times 10^{-4}. \quad (4)$$

The significance of the observed signal is evaluated by $\Sigma = \sqrt{-2 \ln(\mathcal{L}_0/\mathcal{L}_{\text{max}})}$ where \mathcal{L}_{max} and \mathcal{L}_0 denote the maximum likelihood value and likelihood value obtained assuming zero signal events, respectively. The systematic uncertainty is convolved in the likelihood with a Gaussian distribution having a width corresponding to the systematic error of the signal yield. We find the significance of the signal yield to be 3.6σ .

In summary, we have measured the decay $B^- \rightarrow \tau^- \bar{\nu}_\tau$ with $B\bar{B}$ events tagged by semileptonic B decays using a data sample containing 657×10^6 $B\bar{B}$ pairs collected at the $\Upsilon(4S)$ resonance with the Belle detector at the KEKB asymmetric-energy e^+e^- collider. We measure the branching fraction to be $(1.54^{+0.38}_{-0.37}(\text{stat})^{+0.29}_{-0.31}(\text{syst})) \times 10^{-4}$, with a significance of 3.6 standard deviations including systematics. This result is consistent with the previous Belle measurement using $B\bar{B}$ events tagged by hadronic B decays and is consistent with the results reported by the BaBar collaboration. Using the measured branching fraction and known values of G_F , m_B , m_τ and τ_B [16], the product of the B meson decay constant f_B and the magnitude of the Cabibbo-Kobayashi-Maskawa matrix element $|V_{ub}|$ is determined to be

$$f_B |V_{ub}| = (9.3^{+1.2}_{-1.1} \pm 0.9) \times 10^{-4} \text{ GeV}. \quad (5)$$

Using $|V_{ub}| = (3.89 \pm 0.44) \times 10^{-3}$ in Ref. [16], f_B is calculated to be 0.24 ± 0.05 GeV. The measured branching fraction is consistent within errors with the SM expectation from other experimental constraints [3]. The result can be used to extract constraints on new physics models.

We thank the KEKB group for excellent operation of the accelerator, the KEK cryogenics group for efficient solenoid operations, and the KEK computer group and the NII for valuable computing and SINET3 network support. We acknowledge support from MEXT, JSPS and Nagoya's TLPRC (Japan); ARC and DIISR (Australia); NSFC (China); MSMT (Czechia); DST (India); MEST, NRF, NSDC of KISTI, and WCU (Korea); MNiSW (Poland); MES and RFAAE (Russia); ARRS (Slovenia); SNSF (Switzerland); NSC and MOE (Taiwan); and DOE (USA).

-
- [1] The charge-conjugate decays are implied throughout this paper unless otherwise stated.
 - [2] M. Kobayashi and T. Maskawa, Prog. Theor. Phys. **49**, 652 (1973); N. Cabibbo, Phys. Rev. Lett. **10**, 531 (1963).

- [3] J. Charles *et al.* (CKMfitter Group) Eur. Phys. J. C **41**, 1 (2005); Preliminary results as of ICHEP 2010, http://ckmfitter.in2p3.fr/plots_ICHEP10.
- [4] E. Gamiz, C. T. H. Davies, G. P. Lepage, J. Shigemitsu and M. Wingate (HPQCD Collaboration) Phys. Rev. D **80**, 014503 (2009); S. Aoki *et al.* (JLQCD Collaboration) Phys. Rev. Lett. **91**, 212001 (2003); C. Bernard *et al.* (MILC Collaboration) Phys. Rev. D **66**, 094501 (2002); A. Ali Khan *et al.* (CP-PACS Collaboration) Phys. Rev. D **64**, 054504 (2001).
- [5] W. S. Hou, Phys. Rev. D **48**, 2342 (1993).
- [6] S. Baek and Y. G. Kim, Phys. Rev. D **60**, 077701 (1999).
- [7] K. Ikado *et al.* (Belle Collaboration) Phys. Rev. Lett. **97**, 251802 (2006).
- [8] B. Aubert *et al.* (BaBar Collaboration) Phys. Rev. D **77**, 011107(R) (2008).
- [9] B. Aubert *et al.* (BaBar Collaboration) Phys. Rev. D **81**, 051101(R) (2010).
- [10] S. Kurokawa and E. Kikutani, Nucl. Instrum. Methods Phys. Res., Sect. A **499**, 1 (2003), and other papers included in this volume.
- [11] A. Abashian *et al.* (Belle Collaboration), Nucl. Instrum. Methods Phys. Res., Sect. A **479**, 117 (2002).
- [12] Z. Natkaniec *et al.* (Belle SVD2 Group), Nucl. Instrum. Methods Phys. Res., Sect. A **560**, 1 (2006).
- [13] R. Brun *et al.*, GEANT3.21, CERN Report DD/EE/84-1 (1984).
- [14] D. J. Lange, Nucl. Instrum. Methods Phys. Res., Sect. A **462**, 152 (2001).
- [15] E. Barbelio and Z. Wąs, Comput. Phys. Commun. **79**, 291 (1994).
- [16] K. Nakamura *et al.*, J. Phys. G **37**, 075021 (2010).